

# Force Control of a Space Manipulator

Katsuyoshi Tsujita, Kazuo Tsuchiya and Yousuke Kawano

Dept. of Aeronautics and Astronautics,  
Graduate School of Engineering, Kyoto University  
Sakyo-ku, Kyoto 606-8501, JAPAN

**This paper deals with the force control of a space manipulator for a sample-return mission. There are two difficulties in a force control of this class of space manipulator: One is that a space robot has no fixed point in the space and moves when its manipulator exerts a force on the environment. The other is that physical properties of the environment on which the manipulator exerts a force are not well known. In order to overcome these difficulties, a hierarchical controller is proposed in this paper. The controller manages attitude control of the main body and force control of the manipulator. The end effector is attached to the manipulator by a passive compliance mechanism. The performance of the proposed controller is verified by numerical simulations and hardware experiments.**

**Keywords:** Space manipulator, force control

## 1 Introduction

There are two basic subjects for control of a manipulator; trajectory control and force control. For a space manipulator force control can be used at the construction of a space structure. Recently, sample-return missions are receiving attention from space scientists. In such missions, a space robot is sent to an asteroid to sample material and bring it back to the earth. Force control is one of the key technologies of this mission.

So far, a considerable amount of research has been done on force/position control<sup>[1]~[4]</sup>. However,

most of them have dealt with manipulators that are fixed to the ground. Research that has been done on the force control of space manipulators is not not extensive. This paper deals with the force control of a space manipulator for a sample-return mission. There are two difficulties in a force control of this class of space manipulators. One is that the main body of a spacecraft moves when the manipulator exerts a force on the environment. Therefore, motion control of the main body must be also performed when force control is applied to a space manipulator. The other difficulty is that physical properties of the environment on which the manipulator acts a force are not well known. For this reason, force control of a space manipulator must be robust against variations of the physical properties of the environment. In order to overcome the first difficulty, we propose a hierarchical control system which is composed of an attitude controller and a force controller. The attitude controller regulates the attitude of the main body and force controller controls the force acting on the end effector. In general, the motion of the main body of a spacecraft is very slow compared to that of the manipulator. In addition, the motion of the manipulator is also very slow compared to that of the force sensor. Therefore, a control system which has hierarchical architecture that takes each of these time scales into consideration is effective. To overcome the second difficulty, the end effector is attached to the manipulator by a passive compliance mechanism. The passive compliance mechanism can absorb an impulsive force acting on the end effector and align the end effector along an inclined surface.

The performance of the proposed control system is verified by hardware experiments as well as soft-

ware simulations.

## 2 Mathematical model

A space robot composed of a main body and a manipulator with an end effector is considered (Fig. 1). The manipulator is composed of two links, the upper link is connected to the main body through a rotary joint and the lower link is connected to the upper one through a linear joint. The end effector is attached to the lower link by a passive compliance mechanism. An inertial space, the main body, upper and lower links and the end effector are labeled as bodies -1, 0, 1, 2 and 3. For body  $i$ , a unit vector system  $[\mathbf{a}_i]$  is defined.

The following vectors are also defined.

$\boldsymbol{\omega}_{ij} = [\mathbf{a}_i]^T \boldsymbol{\omega}_{ij}$ : Angular velocity vector of  $[\mathbf{a}_i]$  with respect to  $[\mathbf{a}_j]$ .

$\mathbf{r}_i = [\mathbf{a}_i]^T \mathbf{r}_i$ : Position vector from the origin of  $[\mathbf{a}_{i-1}]$  to the origin of  $[\mathbf{a}_i]$ .

$\mathbf{R}_i = [\mathbf{a}_i]^T \mathbf{R}_i$ : Position vector from the origin of  $[\mathbf{a}_i]$  to center of mass of link  $i$ .

$A_{ij}$ : Rotational matrix from  $[\mathbf{a}_j]$  to  $[\mathbf{a}_i]$ .

The cross product of a vector  $\mathbf{x} = [\mathbf{a}]^T x$  is expressed as  $\tilde{x}$  in  $[\mathbf{a}]$ .

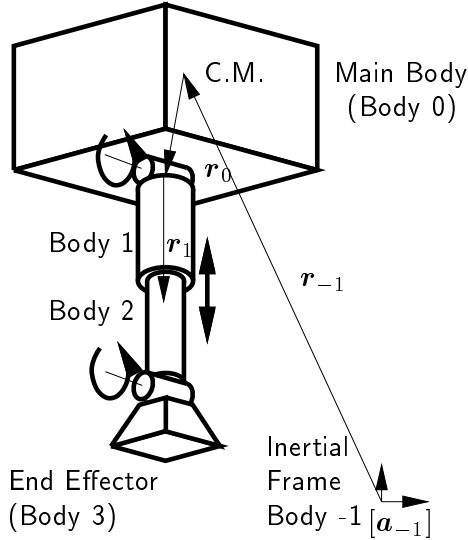


Fig. 1 Schematic model of a space robot

The state variables are defined as

$$z = [\dot{r}_{-1}^T \ \dot{r}_1^T \ \omega_{0-1}^T \ \omega_{10}^T \ \omega_{32}^T]^T \quad (1)$$

Generalized momenta  $L$  concerning to state variable  $z$  are given as follows;

$$L = H\{(\mathcal{L}_r + \mathcal{L}_R)M(\mathcal{L}_r^T + \mathcal{L}_R^T) + J\}H^T z \quad (2)$$

$$\mathcal{L}_r = \begin{bmatrix} A_{0-1}^T & A_{1-1}^T & A_{2-1}^T & A_{3-1}^T \\ O & O & A_{21}^T & A_{31}^T \\ O & \tilde{r}_0^T A_{10}^T & \tilde{r}_0^T A_{20}^T & \tilde{r}_0^T A_{30}^T \\ O & O & \tilde{r}_1^T A_{21}^T & \tilde{r}_1^T A_{31}^T + A_{21}^T \tilde{r}_2^T A_{32}^T \\ O & O & O & O \end{bmatrix}$$

$$\mathcal{L}_R = \begin{bmatrix} O & O & O & O \\ O & O & O & O \\ O & O & O & O \\ O & \tilde{R}_1^T & \tilde{R}_2^T A_{21}^T & O \\ O & O & O & \tilde{R}_3^T \end{bmatrix}$$

$$H = \begin{bmatrix} I & O & O & O & O \\ O & I & O & O & O \\ O & O & I & A_{10}^T & A_{30}^T \\ O & O & O & I & A_{31}^T \\ O & O & O & O & I \end{bmatrix}$$

$$J = \text{diag} [ O \ O \ J_0 \ J_1 + A_{21}^T J_2 A_{21} \ J_3 ]$$

$$M = \text{diag} [ M_0 \ M_1 \ M_2 \ M_3 ]$$

where  $J_0$  and  $J_i$  are the inertia matrix of the main body about the center of mass and that of each link about the center of mass, respectively.  $M_0$  and  $M_i$  are the mass matrices of the main body and each link, respectively.

Equations of motion of generalized momenta  $p_i, l_j$  are derived by Euler-Lagrange formulation as follows;

$$\dot{p}_0 = A_{3-1}^T \lambda_r \quad (3)$$

$$\dot{l}_0 + \tilde{\omega}_0^T l_0 + \tilde{v}_{0r}^T A_{0-1}^T \hat{p}_0 = \tau_0 + E_0 \lambda_r + A_{30}^T \lambda_\theta \quad (4)$$

$$\dot{l}_1 + \tilde{\omega}_1^T l_1 + \tilde{v}_{1r}^T p_1 = \tau_1 + E_1 \lambda_r A_{31}^T \lambda_\theta \quad (5)$$

$$\dot{p}_2 = f_2 + A_{31}^T \lambda_r \quad (6)$$

$$\dot{l}_3 + \tilde{\omega}_3^T l_3 + \tilde{v}_{3r}^T \hat{p}_3 = \tau_3 + \tilde{r}_3^T \lambda_r + \lambda_\theta \quad (7)$$

where  $\tau_i$ , ( $i = 0, 1$ ),  $f_2$  and  $\tau_3$  are input torque, force and passive compliance torque, respectively.  $\lambda_r$  and  $\lambda_\theta$  are reaction force and torque of the kinematical constraints of the end-effector.

$$\begin{aligned} \hat{\omega} &= \begin{bmatrix} \dot{r}_{-1} \\ \dot{r}_1 \\ \hat{\omega}_0 \\ \hat{\omega}_1 \\ \hat{\omega}_3 \end{bmatrix} = \begin{bmatrix} \dot{r}_{-1} \\ \dot{r}_1 \\ \omega_{0-1} \\ A_{10}\hat{\omega}_0 + \omega_{10} \\ A_{31}\hat{\omega}_1 + \omega_{32} \end{bmatrix} \\ v_r &= \begin{bmatrix} v_{0r} \\ v_{1r} \\ v_{2r} \\ v_{3r} \end{bmatrix} = \begin{bmatrix} A_{0-1}\dot{r}_{-1} \\ A_{10}(v_{0r} + \tilde{r}_0\hat{\omega}_0) \\ A_{21}(v_{1r} + \tilde{r}_1\hat{\omega}_1 + \dot{r}_1) \\ A_{32}(v_{2r} + \tilde{r}_2A_{21}\hat{\omega}_1) \end{bmatrix} \\ v_R &= \begin{bmatrix} v_{0R} \\ v_{1R} \\ v_{2R} \\ v_{3R} \end{bmatrix} = \begin{bmatrix} O \\ \tilde{R}_1\hat{\omega}_1 \\ \tilde{R}_2\hat{\omega}_2 \\ \tilde{R}_3\hat{\omega}_3 \end{bmatrix} \\ p &= \begin{bmatrix} p_0 \\ p_1 \\ p_2 \\ p_3 \end{bmatrix} = \begin{bmatrix} M_0v_{0r} \\ M_1(v_{1r} + v_{1R}) \\ M_2(v_{2r} + v_{2R}) \\ M_3(v_{3r} + v_{3R}) \end{bmatrix} \\ \hat{p} &= \begin{bmatrix} p_0 \\ \hat{p}_1 \\ \hat{p}_2 \\ \hat{p}_3 \end{bmatrix} = \begin{bmatrix} p_0 + A_{10}^T\hat{p}_1 \\ p_1 + A_{21}^T\hat{p}_2 \\ p_2 + A_{32}^T\hat{p}_3 \\ p_3 \end{bmatrix} \end{aligned}$$

The above relations are included in the equations of motion with Lagrange multipliers  $\lambda$ .

### 3 Design of a control system

Sample-Return sequence of the space robot is planned to be composed of three stages; The first stage is 'Landing Stage' in which the space robot executes landing maneuver onto the asteroid at very low velocity. The second stage is 'Sampling Stage' in which the end effector touches on the surface of the asteroid and collects material from the surface of the asteroid. In this stage, the end effector needs to be controlled so as to push the surface without

any shock force nor slips. The third stage is 'Take Off Stage.'

In this paper, control system used during the Sampling Stage is considered. The motion of the main body of a space robot, is very slow compared to that of the manipulator. In addition, the motion of the manipulator is also very slow compared to that of the force sensor. In this case, a control system which has a hierarchical architecture that takes each time scale into consideration is effective. Therefore, we propose a hierarchical control system which is composed of an attitude controller and a force controller. The attitude controller regulates the attitude of the main body, and the force controller controls the pushing force acting on the surface of the asteroid to desired value.

The end effector is attached to the manipulator by a passive compliance mechanism which can absorb an impulsive force acting on the end effector and align the end effector along an inclined surface.

Figure 2 shows the architecture of the proposed controller.

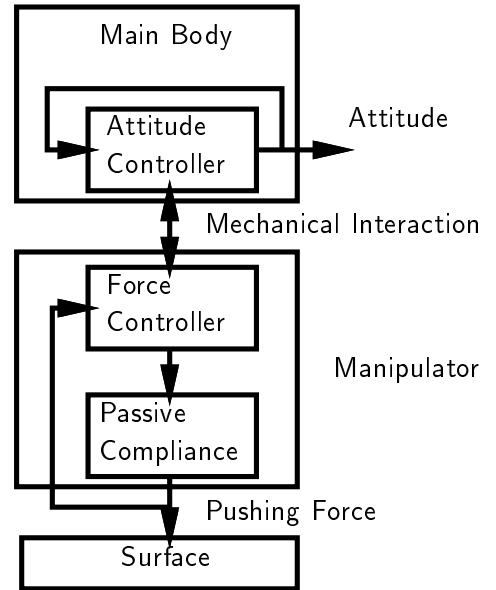


Fig. 2 Architecture of the Controller

#### Design of the Force controller of the linear joint

First, we design a command value of the force

acting on the end effector as follows;

$$f_2 = -K_{p_s}(F_s - F_s^d) - K_{i_s} \int (F_s - F_s^d) dt \quad (8)$$

where,  $K_{p_s}, K_{i_s}$  are feedback gain matrices. Variables  $F_s$  and  $F_s^d$  are the measured value and desired value of the force acting on the surface, respectively.

### Design of the Force Controller of the rotational joint

The commanded torque  $\tau_s^c$  at the joint of the manipulator is calculated as follows;

$$\tau_s^c = J^T \{ -K_{p_s}(F_s - F_s^d) - K_{i_s} \int (F_s - F_s^d) dt \} \quad (9)$$

where,  $J$  is the Jacobian matrix of the manipulator.

### Feedback gains of the Force Controller

Using Eqs.(3) and (5), and eliminating the reaction force from the ground  $\lambda$ , we can get the following equation.

$$K_{44}\dot{\omega}_{10} + h_1 = \tau_1 - J^T \dot{p}_0 \quad (10)$$

where,  $K_{44}$  is a part of the inertia matrix and  $h_1$  is a non-linear term.

Under the assumption that  $\tau_1$  is considered to coincide with the commanded torque  $\tau_s^c$ , and the motion of the main body is considered to be very slow and constant, we can linearize Eq.(10) and get the following equation.

$$K_{p_s}(F_s - F_s^d) + K_{i_s} \int (F_s - F_s^d) dt = 0 \quad (11)$$

Feedback gains are determined based on Eq.(11) under the condition that the manipulator can generate a pushing force at the desired value keeping its stability.

### Design of the Attitude Controller

The attitude controller is designed under the assumption that the pushing force of the end effector is controlled rapidly, and coincides with the desired value well.

First, the required control torques  $\tau_b^c$  for controlling the attitude of the main body are calculated as follows;

$$\tau_b^c = K_{P\theta}(\theta_b^d - \theta_b) + K_{D\theta}(\dot{\theta}_b^d - \dot{\theta}_b) \quad (12)$$

where,  $\theta_b$  and  $\dot{\theta}_b$  are attitude angle and angular velocity of the main body, respectively. Similarly,  $\theta_b^d$  and  $\dot{\theta}_b^d$  are the desired values of attitude angle and angular velocity of the main body.  $K_{P\theta}$  and  $K_{D\theta}$  are position and velocity feedback gains.

### Feedback Gains of the Attitude Controller

Using Eq.(4), and considering that the reaction force  $\lambda$  is controlled to coincide with the constant value  $F_s^d$ , we can get the following equation.

$$K_{33}\dot{\omega}_{0-1} + h_2 = t_0 + (\tilde{r}_0^T A_{0-1} + A_{10}^T J^T) F_s^d \quad (13)$$

where,  $K_{33}$  is a part of the inertia matrix and  $h_2$  is a non-linear term.

Linearizing Eq.(13) and considering that input torque  $t_0$  is controlled to be  $\tau_b^c$ , we obtain the following equation.

$$K_{33}\dot{\omega}_{0-1} = K_{P\theta}(\theta_b^d - \theta_b) + K_{D\theta}(\dot{\theta}_b^d - \dot{\theta}_b) \quad (14)$$

Based on Eq.(14), feedback gains are determined under the condition that the main body keeps a stable attitude.

## 4 Numerical simulation

Performance of the proposed controller is verified by numerical simulations where the space robot approaches the inclined surface (10 [deg]) of the asteroid at a velocity of 1.0 [cm/s] and exerts a pushing force perpendicular to the surface for a certain time period. **Table 1.** shows the physical parameters. Figure 3 shows the pushing force exerted on the surface and **Fig. 4** shows the position of the main body and the end effector. These figures indicate that the proposed control system established a constant desired pushing force without any shock forces nor slips of the end effector and from the target point.

**Table. 1.** Parameters

Space Robot		
Main Body		
Mass	$3.28 \times 10^2$	[kg]
Inertia	138, 65.0, 134	[kg m <sup>2</sup> ]
Link 1		
Mass	1.70	[kg]
Inertia	0.00362, 0.00441, 0.00362	[kgm <sup>2</sup> ]
Link 2		
Mass	2.86	[kg]
Inertia	0.0337, 0.0337, 0.00418	[kgm <sup>2</sup> ]
Asteroid		
Inclination	10	[deg]

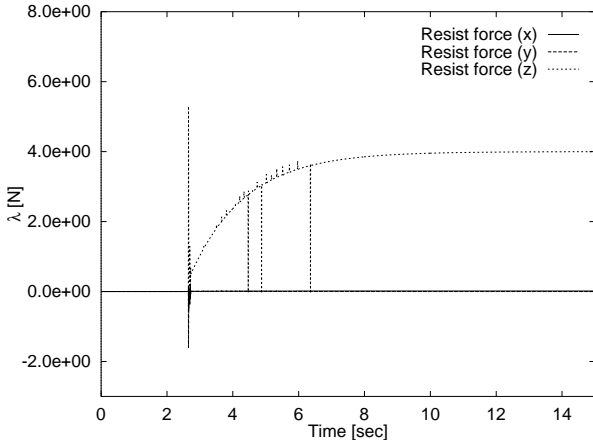


**Fig. 3.** Reaction Force Vertical to the Surface

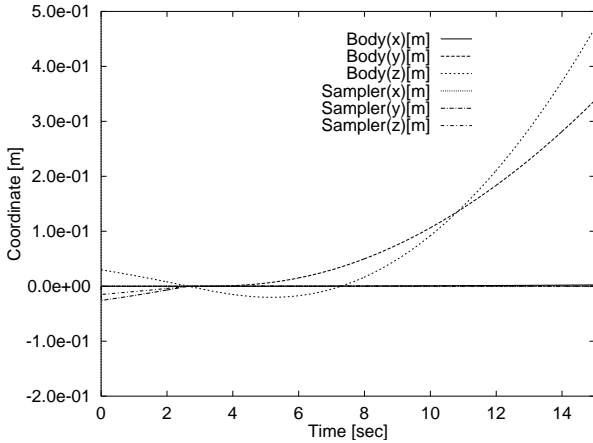


**Fig. 4.** Position of the Main Body and the End Effector

## 5 Hardware simulation

The performance of the proposed controller is also verified by hardware simulation. The hardware simulations are done using a 'simulator-table' with 9 degrees of freedom(DOF) that can simulate the motion of the main body of the robot in free space. The space manipulator is mounted on the 'simulator-table' and controlled by the force controller using angle-sensor and force-sensor signals from the manipulator. On the other hand, the simulator-table was programmed to simulate the mathematical model of the robot with inputs from the force-sensor signal. Figure 5 shows the architecture of the hardware equipment.

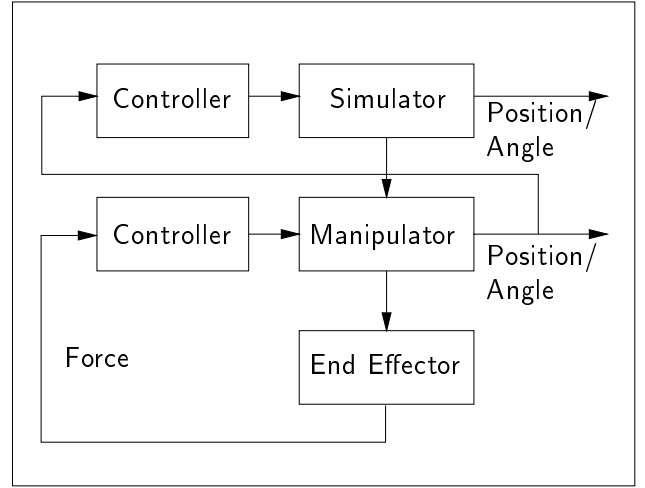


**Fig. 5.** The Architecture of Hardware Equipment

Figures 6 and 7 show the results of the hardware experiments where the space robot approaches the inclined surface(10 [deg]) of the asteroid at a velocity of 1.0 [cm/s] and exerts the pushing force perpendicular to the surface for a certain time period. The time history of the position of the main body and the end effector are shown respectively. It can be seen that the end effector can push the inclined surface of the asteroid without slips.

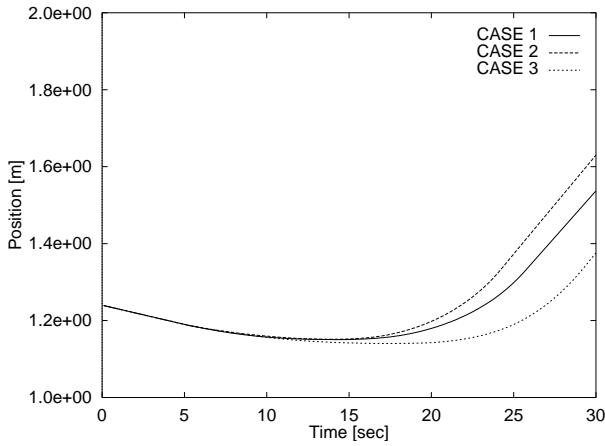


Fig. 6. Position of the main body

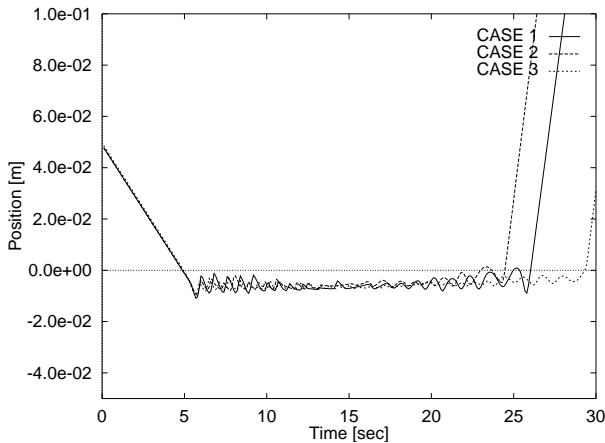


Fig. 7. Position of the end effector

## 6 Conclusions

In this paper, force control of a space robot is treated. The control system proposed here is composed of an attitude controller for the main body of a space robot and a force controller for the end effector which has passive compliance. Performance of the control system is verified through numerical simulations and hardware simulations. The proposed controller established a stable pushing force at the end effector that was at the desired value. The end effector was not exposed to shock forces nor slips from the target point.

## Acknowledgment

This research, especially the experimental study was accomplished using a simulator-table in The Institute of Space and Aeronautical Science (ISAS, Japan). The authors wish to acknowledge the assistance of Prof. Kawaguchi, Prof. Nakatani and staff of the ISAS.

## References:

- 1) R.E.Goddard, Y.F.Zheng and H.Hemami: Dynamic Hybrid Velocity/Force Control of Robot Compliant Motion over Globally Unknown Objects, IEEE Transactions on Robotics and Automation, Vol.8, No.1, pp. 132-138, (1992)
- 2) T.Yoshikawa and A.Sudou: Dynamic Hybrid Position/Force Control of Robot Manipulators—On-Line Estimation of Unknown Constraint, IEEE Transactions on Robotics and Automation, Vol.9, No.2, pp. 220-227, (1993)
- 3) D.Wang and N.H.McClamroch: Position and Force Control for Constrained Manipulator Motion: Lyapunov's Direct Method, IEEE Trans. on Robotics and Automation, Vol.9, No.3, pp. 308-313, (1993)
- 4) D.Jeon and M.Tomizuka: Learning Hybrid Force and Position Control of Robot Manipulators, IEEE Transactions on Robotics and Automation, Vol.9, No.4, pp.423-431, (1993)